

# Special Purpose Ammonia Frequency Standard—A Feasibility Study

DAVID J. WINELAND, DAVID A. HOWE, MICHAEL B. MOHLER,  
AND HELMUT W. HELLWIG, SENIOR MEMBER, IEEE

**Abstract**—We have investigated the feasibility of a special purpose frequency standard based on microwave absorption in ammonia gas ( $N^{15}H_3$ ). Such a device would potentially fill a need in certain communications and navigation applications for an oscillator which has medium stability, greater accuracy ( $\sim 10^{-9}$ ) than that provided by crystal oscillators, but a cost significantly smaller than that of more sophisticated atomic frequency standards. A device was constructed using a stripline oscillator near 0.5 GHz whose multiplied output was frequency-locked to the absorption of the 3-3 line in  $N^{15}H_3$  ( $\sim 22.8$  GHz). Output between 5 and 10 MHz was provided by direct division from the 0.5-GHz oscillator. Observed stability was  $2 \times 10^{-10}$  from 10 to 6000 s, and reproducibility (accuracy) is estimated to be  $\pm 2 \times 10^{-9}$ . The unique features of this device, which include 1) high-performance stripline oscillator, 2) digital servo techniques, 3) unique oscillator-cavity servo, 4) pressure shift compensation scheme, and 5) acceleration insensitivity, are discussed. Areas for further study are noted.

## I. INTRODUCTION

THE SPECIAL purpose ammonia frequency standard has grown out of a need for a frequency standard satisfying specific requirements not found in other precision oscillators. Briefly, these currently available oscillators can be divided into two classes: the quartz-crystal oscillators and atomic "clock" oscillators. The quartz-crystal oscilla-

tors, while having good short-term stability and low cost ( $\sim \$500$  to  $\sim \$2000$ ) suffer three major drawbacks: 1) The frequency is not invariant between units and is related to the macroscopic parameters such as the dimensions of the quartz crystal. Therefore, calibration is required initially and subsequent recalibration is required due to "aging" of the crystal. 2) The crystal oscillator is sensitive to vibration and shock. These environmental factors affect the macroscopic dimensions of the crystal, and therefore can cause step shifts in frequency. 3) The quartz-crystal oscillator is temperature dependent and when oven-controlled requires long warm-up time.

Atomic oscillators provide stabilities from one part in  $10^{10}$  to one part in  $10^{13}$  per year. Their cost ranges from approximately \$4000 to above \$20 000 depending upon performance. Their excellent frequency stability and intrinsic accuracy make recalibration unnecessary for most applications, however this higher level of performance is not needed in many applications. In addition, their warm-up time is generally long and their performance under severe environmental conditions (acceleration, vibration, temperature, barometric pressure, and magnetic fields) is inadequate in some cases.

Presently there exists a need in many communication and navigation systems applications for low-cost oscillators with accuracy better than that provided by crystal oscillators, but not as high as available atomic standards. With these needs in mind, we investigated the possibility of constructing an oscillator with  $10^{-9}$  accuracy and  $10^{-10}$  stability, which could also be made environmentally insensitive, have quick warmup and the potential for small size, weight, power consumption and low cost.

Manuscript received February 13, 1978; revised November 27, 1978 and February 26, 1979. This work was supported by the Advanced Projects Agency of the Department of Defense and was monitored by ARPA under Contract # 3140.

D. J. Wineland, D. A. Howe, and M. B. Mohler are with the Frequency and Time Standards Section, National Bureau of Standards, Boulder, CO 80302.

H. W. Hellwig was with the Frequency and Time Standards Section, National Bureau of Standards, Boulder, CO. He is now with Frequency and Time Systems, Inc., Danvers, MA.

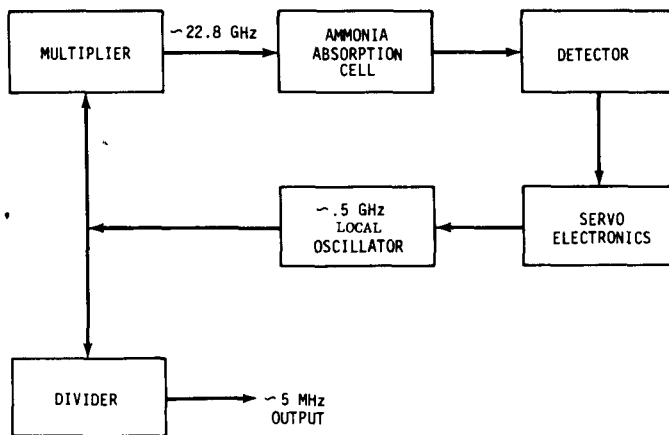


Fig. 1. Simplified block diagram of system. Frequency lock servo is used employing 0.5–25 kHz FM on  $\sim 0.5$ -GHz oscillator.

In order to meet the above requirements we looked for a system which incorporated the desirable features of both the atomic oscillators (high accuracy, stability) and crystal oscillators (low cost) and included features of environmental insensitivity and fast warm-up. Since neither ultimate accuracy nor stability is required for these applications, sacrifices could be made in this regard. After careful consideration (see Section IV) the 3-3 inversion transition in ammonia  $N^{15}H_3$  gas was chosen as a frequency reference. As shown in Fig. 1, the system is a passive device using gas cell absorption [1]; it is not a "maser." Unlike a beam device, it is therefore subject to full Doppler broadening. Historically, this gas cell absorption scheme was used in the first "atomic" clock in 1948 [2]. Active research on this basic device was pursued until about 1955, but was slowed down because other more promising devices, such as those based on atomic beams, although more complicated, provided better accuracies and stabilities than those which could be obtained from simple gas cell devices. In 1954, the accuracy of such an ammonia device [3] was about 5 parts in  $10^8$  with approximately 1 part in  $10^8$  stability and the apparatus was quite complicated and expensive, suitable only as a laboratory instrument. However, since that time, vast improvements have been made in RF and microwave electronics; these, coupled with new insights into the electronic and physical problems encountered, suggested that the ammonia absorption cell could be used to provide the "special purpose" oscillator described above.

In Fig. 1 a local oscillator is referenced to the 3-3 transition in  $N^{15}H_3$  (22.79 GHz). For simplicity the frequency of the local oscillator is chosen so that in one step it can be multiplied to the ammonia frequency, and at the same time it can be directly divided to the oscillator output frequency near 5 MHz, which is harmonically related by a factor of 4400 to the ammonia frequency. The oscillator is a simple stripline oscillator, the multiplier uses a waveguide mounted step recovery diode, and the dividers are readily available integrated circuit (IC) modules.

Below we discuss the system and the results obtained. It is convenient to cover first the main components of the system:

Oscillator and divider, multiplier, ammonia cell and microwave cavity, and servo system. Then we discuss ammonia cell development results obtained on stability, accuracy (reproducibility), and sensitivity to environmental parameters. Finally, we note future possibilities based on our present results.

## II. LOCAL OSCILLATOR ( $\sim 0.5$ GHz) AND DECADE DIVIDERS

In reviewing the possible oscillator designs, it appeared that an oscillator using a simple *LC* resonator should be investigated. Advantages to this design include:

- 1) wide tunability,
- 2) continuous operation under very adverse condition (shock, vibration),
- 3) good short-term stability,
- 4) low cost.

We developed an oscillator operating at about 0.5 GHz and having a free-running stability as shown in Fig. 2. The curves were obtained including a divider chain ( $\div 100$ ) after the 0.5-GHz oscillator. These data were computed using the two sample variance for different averaging times [4], however, frequency drift was not removed. The bandwidth of the measurement system affects the variance in the case of white and flicker of phase type noise; therefore, two curves with different bandwidths are plotted around the averaging times of interest ( $\sim 10$  ms). The oscillator features an etched strip on a printed circuit (PC) board as a transmission line resonator (stripline resonator). In the design of a high-performance stripline oscillator, we must address three principal problems [5]:

- 1) minimization of resonator losses,
- 2) minimization of additive transistor noise,
- 3) isolation of the resonator from shock and vibration.

Radiative loss is minimized by adopting a three-layer sandwich etch technique. In this design, two ground planes are used on the top and bottom surfaces of the PC board with the stripline centered between the dielectric. To keep loss to a minimum, fiberglass-*teflon* which has a loss tangent of about  $10^{-3}$  is used for the dielectric. The stripline is a 7-cm length of copper, 1 cm wide and 2 mm thick. Silver-solder is used on all connections to minimize contact resistance. The unloaded  $Q$  of the resonator at 0.5 GHz is about 400. Loaded  $Q$  of the resonator is maximized by the use of field-effect transistor (FET) as the active element [6]. The FET is chosen to have a high forward transconductance and a high cutoff frequency.

Oscillator noise behavior is generally characterized by low-frequency (near carrier) flicker noise and high-frequency (far from carrier) white-phase noise which may be multiplicative or additive. Causes of flicker behavior are difficult to identify, but careful selection of a transistor which is manufactured with care in a clean environment may reduce the flicker noise, since it has been related to sporadic conductance through the device due to impurities. White-

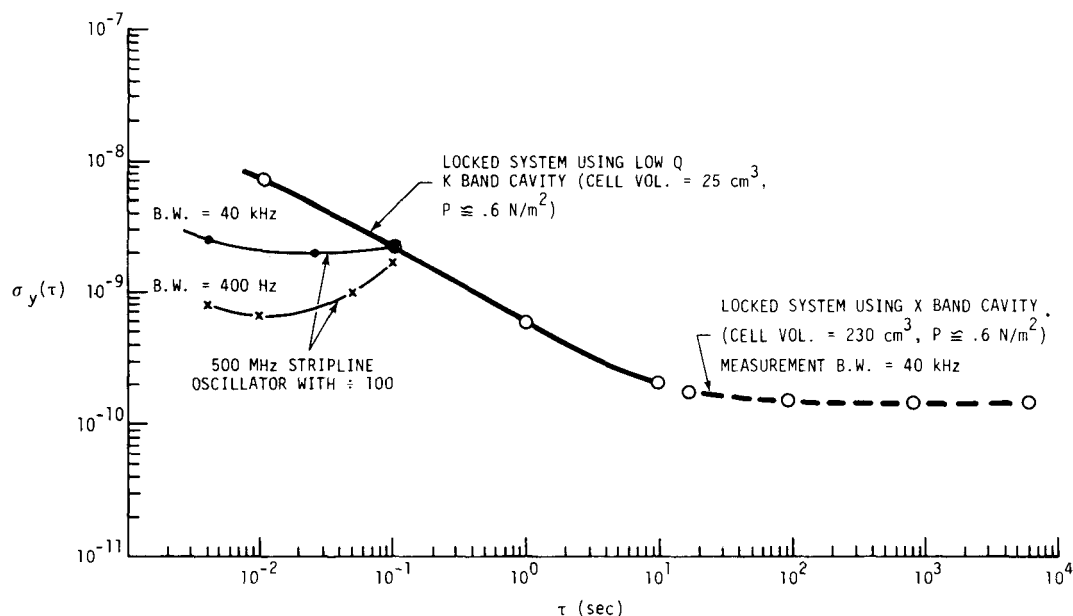


Fig. 2. Frequency stability plots showing the two sample variance ( $\sigma_y$ ) for different averaging times ( $\tau$ ). BW  $\equiv$  measurement system bandwidth.

phase noise is usually associated with additive thermal noise of components and/or transistor parameters. We could resort to devices capable of higher signal levels in order to get above a fixed noise level. Since higher device currents usually aggravate the flicker-noise problem, a tradeoff exists between white phase noise and flicker noise. We have arrived at a compromise solution which gives suitable performance in the ammonia standard. The curves shown in Fig. 2 represent a higher device drive level than is common in, for example, quartz crystal oscillators.

At frequencies around 0.5 GHz, transistor package parameters (inductance and capacitance) and stray parasitic elements such as connecting lead inductance and stray capacitance all contribute substantially to the fundamental resonance. If we want to achieve a relative frequency stability approaching  $1 \times 10^{-9}$ , then it is imperative to maintain resonator inductance and capacitance values stable to this level. In an LC oscillator the greatest difficulty in design is to achieve high inductive and capacitive stability. We reduced the problem of vibration induced microphonics by using a three-layer PC board and mounting rigidly all components using a low loss doping compound. The oscillator is in turn rigidly fixed to an aluminum block which acts as the shield for the components. The test block weighs about 3 kg. When rigidly mounted, structure-borne vibration is directly applied to the oscillator. A soft mount designed to isolate the oscillator from vibration can reduce the transmitted vibration at higher frequencies at the expense of increasing the vibration sensitivity at a lower frequency.

The vibration sensitivity of the local oscillator is significant in cases of shock and vibration where the period of the vibration is shorter than the servo loop time constant. However, since the ammonia resonance has a line width of approximately 100 kHz, a shorter loop time constant can be

used. More specifically, if the unity gain point for the servo system is designed to be 50 kHz, and a second-order servo loop is used, the gain  $G$  of the servo for frequencies  $\nu$  less than 50 kHz is  $G \approx (50 \text{ kHz}/\nu)^2$ . Therefore, assuming that the observed ammonia resonance is vibration insensitive, the vibration sensitivity of the locked oscillator at lower frequencies is reduced by this factor (at 50 Hz this reduction would be a factor of  $10^6$ ). Therefore, the design of the oscillator mount should yield a vibration response in which the higher frequencies are suitably attenuated (see Section VI-F).

The division from 500 MHz to 5 MHz uses an emitter-coupled logic (ECL) decade divider followed by a transistor-transistor logic (TTL) decade divider (from 50 MHz to 5 MHz). A level translator was used between these IC's. The ECL divider contained an internal wideband amplifier, thus allowing good isolation between divider logic and the source. In short term ( $< 10 \text{ ms}$ ), the white phase noise of the dividers set a limit on the stability at 5 MHz.

### III. STEP-RECOVERY DIODE MULTIPLIER

For the frequency multiplier, the  $Q$  was kept low ( $< 10$ ) in order to reduce frequency to amplitude conversion. We also required a power output of at least  $5 \mu\text{W}$ . For this reason, we used low-capacitance step-recovery diodes in a waveguide multiplier module [1], [7]. Briefly, the most difficult problem was one of impedance matching for both the input and output circuit. For example, for the input circuit ( $\sim 0.5 \text{ GHz}$ ) the dynamic diode impedance was  $Z \approx 1 \Omega$ . Therefore, two  $\pi$  section transformers were cascaded to match to the  $50\text{-}\Omega$  output impedance of the 0.5-GHz amplifier. Approximately 0.5-W input power was needed to "snap" the diode properly. To accomplish this, a microstrip hybrid class "C" amplifier was used. The amplifier, microstrip

matching circuit and multiplier module were integrated into one package in order to avoid instabilities due to connections. The output circuit was composed of a shorting stub and iris coupling to form a cavity ( $Q \approx 10$ ) with the diode approximately matched to the characteristic impedance of the narrow height waveguide. In the interest of rigidity and simplicity, shims were used rather than movable plungers. With  $\sim 0.6$ -W input power to the diode, output power of approximately 100  $\mu$ W was obtained at 22.79 GHz [1].

#### IV. AMMONIA-GAS ABSORPTION CELL

The advantages of using ammonia as the reference (quantum mechanical) resonator are:

1) The microwave transition of interest (3-3 inversion line) provides an absorption signal which is orders of magnitude stronger than those of other interesting molecules or atoms [8], [9]. This is a significant advantage because it means that the desired signal-to-noise ratio is obtained without resorting to impractically large microwave cells as would be necessary for other gases.

2) Since ammonia remains in the gas phase for the temperature range of interest ( $-40^\circ\text{C}$  to  $+60^\circ\text{C}$ ) the device has instant turn on capability. One must, however, note the existence of a pressure- (therefore, temperature-) dependent frequency shift; this is discussed more fully below.

3) The frequency of the ammonia transition is fundamental in nature and therefore essentially eliminates the need for calibration of the device.

4) The ammonia transition linewidth is fairly broad ( $\sim 100$  kHz). This is a disadvantage in terms of the ultimate accuracy obtainable, but it allows the primary oscillator to be locked to the ammonia reference in very short times ( $\gtrsim 15$   $\mu$ s). This potentially allows a significant reduction in the acceleration sensitivity of the local oscillator.

##### A. Choice of $\text{N}^{15}\text{H}_3$

We chose the 3-3 line in ammonia because of its large signal strength. The  $\text{N}^{15}\text{H}_3$  isotope was chosen because the  $\text{N}^{15}$  nucleus has no quadrupole moment and therefore it is free from the quadrupole structure which makes the 3-3 line of the  $\text{N}^{14}\text{H}_3$  isotope asymmetric. This asymmetry causes the apparent line center of  $\text{N}^{14}\text{H}_3$  to depend on FM modulation amplitude and microwave power; uncertainties as large as approximately  $4 \times 10^{-8}$  could be expected from this asymmetry.

The results of three high-resolution determinations of the 3-3,  $\text{N}^{15}\text{H}_3$  frequency are:

$$\nu_0 = 22\,789\,421\,698 \pm 3 \text{ Hz [10]}$$

$$\nu_0 = 22\,789\,421\,701 \pm 1 \text{ Hz [11]}$$

$$\nu_0 = 22\,789\,421\,672 \pm 55 \text{ Hz [12].}$$

These measurements were taken with ammonia-beam masers and show that although rather high resolutions can be obtained, a conservative estimate of uncertainty in the frequency is about  $2 \times 10^{-10}$ ; for our work we, therefore, assumed  $\nu_0 = 22\,789\,421\,700$  Hz.

##### B. Containment of Ammonia

Most aspects of the present device were tested in an experimental apparatus using a gas-flow system for the ammonia [1]. A simple gas-flow system could be used in a prototype device but the added complexity is a disadvantage. Therefore, we found it desirable to develop permanent closed cells.

The problem of ammonia containment is well known; in a simple cell using brass or copper waveguides, reaction of ammonia with the cell walls causes rapid disappearance of the signal particularly if water vapor is present. Also, chemisorption with certain metals is noted [13]. Various inert cell coatings were considered [1], however, we felt that a simpler approach would be to make cells from inert materials whose cleanliness could be ensured.

Two basic problems were encountered in obtaining these cells: 1) provision had to be made for evacuating, baking, and sealing the cells, 2) the cells had to form part of, or be included in a microwave cavity for interrogation by the microwave radiation. This implied that the material used for the windows must be nearly lossless and be easily bonded to the rest of the cavity. Two basic schemes were tried and, although more work is needed, the results are encouraging.

Our first cells were made with quartz cylinders of rectangular cross section which could be inserted into X-band waveguide. Both ends were extended and drawn into points to provide a seal. Quartz was used because its microwave losses are negligible. The cells were baked under vacuum at  $300^\circ\text{C}$  for 30 h at a pressure of  $< 10^{-4}$  Pa (1 torr  $\approx 133$  Pa). Ammonia was then backfilled at pressures between 0.13 and 0.67 Pa ( $10^{-3}$  torr to  $5 \times 10^{-3}$  torr). No attempt was made to purify the ammonia which was contained in a lecture bottle and admitted to the cell through a metal leak valve. The cells were then sealed by heating a quartz pinchoff.

We constructed a second type of cell made of stainless steel K-band waveguide. Windows were made of quartz and were mated to brass flanges with pressed indium seals. A copper pinchoff was silver soldered to the broad face of the waveguide in which small holes were drilled. The other end of the pinchoff was connected to a vacuum system and the waveguide was evacuated. The cells were baked at  $100^\circ\text{C}$  for 50 h at a pressure of  $< 10^{-4}$  Pa. The ammonia gas was backfilled through the vacuum system to waveguide (without purification) and the copper pinchoff was then sealed.

Conceptually, the simplest approach for locking the local oscillator to the ammonia transition is to pass the microwaves through the ammonia cell and servo the frequency of the oscillator to the point of maximum absorption. No errors would occur with this method if there were no reflections at the ammonia cell interface and if the source and detector were perfectly matched to the microwave guide. Such is hardly the case in practice, and since reflections occur at both sides of the ammonia cell, it is effectively contained in a cavity.

Frequency pulling due to cavity mistuning is a familiar problem to designers of atomic clocks. In a passive standard such as the one discussed here, the frequency  $\nu$  at which

microwave absorption is maximum is given by [14]:

$$(v - v_0) = \frac{Q_c}{Q_t} (v_c - v_0) \quad (1)$$

where

- $v_0$  unperturbed ammonia frequency,
- $v_c$  cavity center frequency,
- $Q_c$  microwave cavity  $Q$ ,
- $Q_t$  ammonia transition  $Q$ ,

and the expression is valid when:

$$(v_c - v_0)/v_0 \ll 1/Q_c, Q_t \gg Q_c.$$

This result obtains because the ammonia and microwave cavity form a system of coupled resonators. Qualitatively, varying the frequency of the cavity changes the apparent frequency of the ammonia transition. In a cavity formed from a section of waveguide the importance of reflections is illustrated by the following example: If we made an ammonia cell from a section of copper WR-42 waveguide of length  $l$  and if the windows have (real) voltage reflection coefficients of value  $\Gamma_v$ , then the effective  $Q$  of the resulting cavity can be shown to be

$$Q_c = \frac{2\pi l \lambda_g \Gamma_v}{\lambda_0^2 (1 - \Gamma_v^2)} \quad (2)$$

where

- $\lambda_g$  guide wavelength,
- $\lambda_0$  free-space wavelength.

If we choose  $\Gamma_v = 0.2$ ,  $l \approx 50$  cm [15] and since  $\lambda_g \approx 1.59$  cm,  $\lambda_0 = 1.31$  cm at the frequency of interest then  $Q_c \approx 57$ . From (1), we find that we would have to tune the cavity to 0.04 percent of its linewidth to obtain  $10^{-9}$  accuracy in the output frequency. Since the expansion coefficient  $\alpha$  for copper is  $1.5 \times 10^{-5}/^\circ\text{C}$  and  $Q_t \approx 2 \times 10^5$  then the frequency dependence on temperature due to cavity pulling would be

$$\frac{1}{v_0} \frac{\partial v}{\partial T} = \frac{Q_c}{Q_t} \alpha \approx 10^{-8}/^\circ\text{C}.$$

Because of this rather strong sensitivity and because it is difficult to make reflectionless windows for the cavity, we servoed the cavity to line center. A few possibilities exist for accomplishing this. First, we could separately sense the cavity frequency with microwave power applied symmetrically to either side of the cavity resonance [16]. However, frequency-to-amplitude conversion is a severe problem with the low cavity  $Q$  obtained here, and such a method was prohibited. Secondly, we could look for zero change in output frequency when the  $Q_t$  is varied; this assures  $v_c - v_0 = 0$  in (1). This could be accomplished by symmetrically broadening the line by applying a magnetic field [3]. Unfortunately, this broadening is only  $\sim 7$  MHz/T (1 Gauss =  $10^{-4}$  Tesla) and therefore, a rather large magnetic field is required to broaden the line appreciably. Another disadvantage of this scheme is that it requires a second

reference oscillator in order to detect frequency changes when the magnetic field is changed. A third method exists and, to the authors' knowledge, has not been used previously. It is discussed in the next section.

## V. SERVO SYSTEM

The basic requirement of the servo system is that it force the frequency of the local oscillator ( $\sim 0.5$  GHz) to be at a subharmonic of the ammonia transition frequency. Of course, various systematic effects shift the apparent frequency of the ammonia transition; these must either be eliminated or controlled in a known way. Although the performance of the present device was not high when compared to a state-of-the-art atomic clock, the demands on the servo system are rather high. This is because we are trying to servo to the center of the rather broad ammonia resonance feature (i.e., split the linewidth) to about  $10^{-5}$  or 0.001 percent of the linewidth. Therefore, state-of-the-art techniques had to be employed. Below we discuss the effects of cavity pulling, distortions in the source and detector and servo offsets and drifts. Quite generally, these effects change the apparent center position of the transition and, since the magnitude of the effects can change in time, both accuracy and stability are limited.

### A. Cavity Pulling

To separate out the effects of cavity pulling, first assume that the microwave source and detector are perfectly flat, that is, the power output from the source and the detected power do not depend on frequency; the more general case is discussed below. Equation (1) yields the frequency  $v$  where the absorption is a maximum. To facilitate the detection of this condition, source frequency modulation was used. This technique is well known and is used in other atomic clocks, including those based on cesium, rubidium, and hydrogen [16], [17]. Basically, the source frequency is modulated at frequency  $v_m$  so that the time dependence of the microwave field from the source is:

$$E = E_0 \cos \left( \omega_s t + \frac{\Delta\omega}{\omega_m} \cos \omega_m t + \phi \right),$$

where

- $\omega_s$   $2\pi v_s$  (average frequency of source),
- $\Delta\omega$  peak frequency excursion,
- $\omega_m$   $2\pi v_m$  (angular modulation frequency),
- $\phi$  arbitrary phase angle,
- $\Delta\omega/\omega_m$  modulation index.

When  $v_s - v_0 \approx \Delta v_t$  ( $\Delta v_t =$  ammonia linewidth) the detected signal will have an oscillating component at frequency  $v_m$ ; the phase and amplitude of this component will vary as a function of frequency as shown in Fig. 3(a). This "dispersion" curve can be used to servo the primary oscillator to the apparent line center by finding the condition where the dispersion curve is zero. When  $\Delta\omega \ll 2\pi\Delta v_t$ , the frequency at which this occurs is given by (1). However, for  $\Delta\omega \approx 2\pi\Delta v_t$ , equation (1) must be slightly modified as

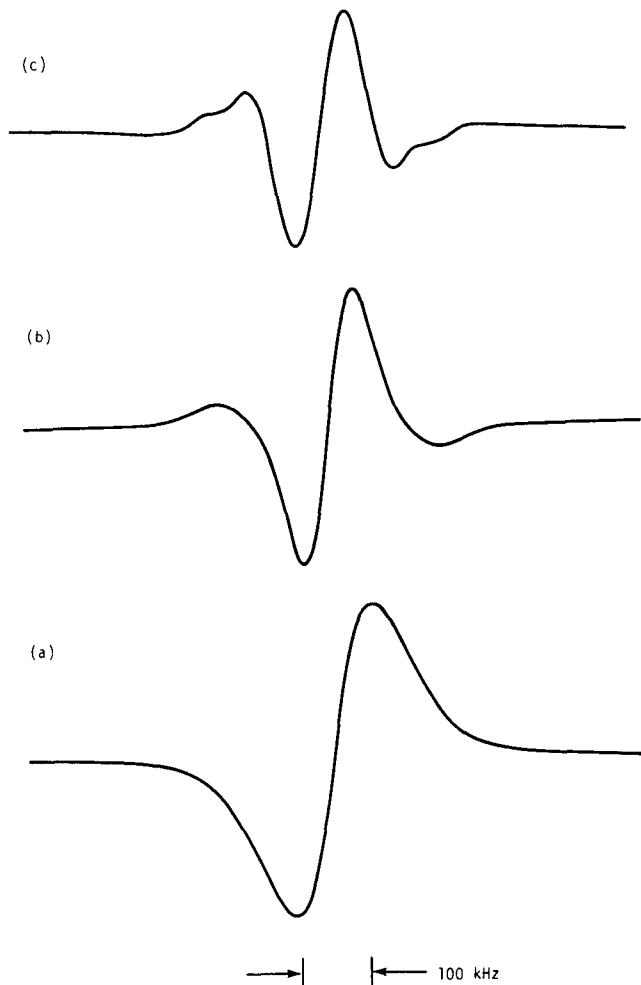


Fig. 3. Dispersion curves obtained at output demodulator for different harmonics: (a) Fundamental. (b) Third harmonic. (c) Fifth harmonic. Vertical scales are different in the three cases.

discussed below. Also we note the appearance of higher harmonics of  $\nu_m$  in the detected output; in particular, the amplitudes and phases of the higher odd harmonics have similar "dispersion" characteristics. Fig. 3(b) and (c) show the measured dispersion curves for the third and fifth harmonics, respectively, when  $\Delta\omega$  is adjusted to give maximum slope near the center of the pattern. These curves are the voltages observed at the outputs of the mixers in Fig. 4 when the feedback loops are open. Therefore we could use the dispersion curves of the higher odd harmonics to lock to line center. Two important points should be made:

1) For large modulation amplitudes  $\Delta\omega \cong 2\pi\Delta\nu_l$  it can be shown that (1) is modified to the form:

$$\nu - \nu_0 = K(n) \frac{Q_c}{Q_l} (\nu_c - \nu_0) \quad (3)$$

where  $K(n)$  is close to unity but varies by factors of two or three as  $\Delta\omega$  is varied. It is also a function of the harmonic number observed ( $n$ ) and in general  $K(n) \neq K(n')$  for the same  $\Delta\omega$ . We used this property to simultaneously servo the oscillator and cavity to line center, therefore eliminating cavity pulling. As shown in Fig. 4, the third harmonic

dispersion was used to lock the multiplied primary oscillator to apparent line center, i.e., the condition:

$$\nu - \nu_0 = K(3) \frac{Q_c}{Q_l} (\nu_c - \nu_0) \quad (4)$$

was satisfied. The fifth-harmonic dispersion was used to lock the cavity to the line center, i.e., the condition:

$$\nu - \nu_0 = K(5) \frac{Q_c}{Q_l} (\nu_c - \nu_0) \quad (5)$$

was satisfied. Since  $K(3) \neq K(5)$ , conditions (4) and (5) could be satisfied simultaneously only if  $\nu_c - \nu_0 = \nu - \nu_0 = 0$ .

2) The use of the above scheme causes some loss of signal strength. To give an idea of this loss we measured the ratio of the slopes [ $SL(n)$ ] of the dispersion curves when the microwave power was kept fixed and when the slope was maximized by adjusting  $\Delta\omega$  for each harmonic. We measured

$$SL(1):SL(3):SL(5) = 1.0:0.42:0.26.$$

From the standpoint of signal strength it would be better to use the fundamental and third harmonic locks in the above scheme; however, conditions (outlined later) led us to choose the third- and fifth-harmonic locks. We note that a further slight reduction in signal strength or slope ( $\cong 10$  percent) is observed when the system is optimized for the third and fifth harmonic locks simultaneously.

The microwave cavity is formed by a combination of shunt impedances due to the windows and added reactances at both ends of the ammonia cell. Electronic tuning is provided by a varactor diode at one end of the cell.

### B. Distortions in the Microwave Source and Detector

In general, the source and detector are not "flat" with frequency; that is, frequency-to-amplitude conversion occurs which shifts the apparent frequency of the ammonia transition. The most serious problem occurs in the source. Briefly, frequency-to-amplitude conversion occurs because of the (slightly mistuned) reactances in the source. This causes the apparent ammonia frequency to shift due to two effects: 1) In time domain, a qualitative picture of the first effect is given by assuming that as the frequency of the source swings below  $\nu_0$ , its output power increases; as its frequency swings above  $\nu_0$ , its output power decreases. Assuming that  $\nu_c = \nu_0$ , and  $\nu_s = \nu_0$ , then the signal from the ammonia absorption would be stronger when  $\nu_s$  was on the low side of  $\nu_0$  than on the high side. Equivalently, there exists a residual signal component at  $\nu_m$  (and  $3\nu_m$  and  $5\nu_m$ ) on the detector which the servo must then compensate for by shifting  $\nu_s$  to a value below  $\nu_0$ . Since  $\Delta\omega/2\pi \cong \Delta\nu_l$  in practice, then if AM of amplitude  $\beta$  exists due to frequency-to-amplitude conversion, we would have:

$$(\nu_s - \nu_0) \cong -\beta\Delta\nu_l \quad (6)$$

in the locked condition. 2) The second effect occurs predominantly only for the fundamental dispersion lock (at  $\nu_m$ ). The effect is due to the AM signal component (at frequency

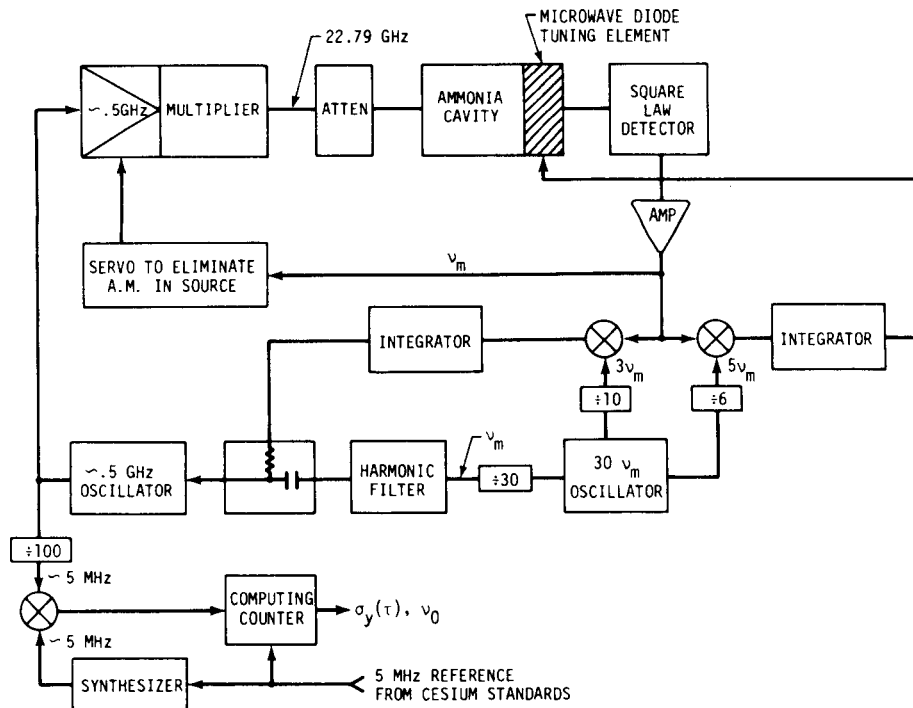


Fig. 4. Detailed block diagram of system.

$v_m$ ) observed at the detector which is *not* due to ammonia absorption, but is due to direct transmission of microwave power. If the signal from the ammonia is only a small fraction ( $\gamma$ ) of the total signal reaching the detector, the frequency lock point due to this effect is given by

$$(v_s - v_0) \approx \frac{\beta}{\gamma} (\Delta v_l) \quad (\text{fundamental lock}).$$

However, for the third- and fifth-harmonic locks, this second effect is reduced and (6) applies to a high degree because the third and fifth harmonics appear at the detector only because of the presence of ammonia. This is one reason for using the higher harmonic locks.

If the source is "flat" with frequency and the detector is not, the problem is less severe. Since we are locking to the third and fifth harmonics of  $v_m$  then the spurious third- or fifth-harmonic signal is generated only because the curvature (nonlinearity) of the detector converts the FM (at frequency  $v_m$ ) into AM at frequency  $3v_m$  or  $5v_m$ . Since the curvature of the detector should be small this type of offset should be negligible. This is the second reason for using the third- and fifth-harmonic locks as noted in Section V-A. Third harmonic lock of the primary oscillator [18] also discriminates against background slopes (for example, due to overlapping transitions) but this is not a problem for the ammonia device.

In general, it is easier to control the frequency-to-amplitude slope of the detector than it is for the source. Therefore, we servoed out the AM (at frequency  $v_m$ ) in the source by nulling the signal (at  $v_m$ ) observed at the detector. Since the detector may not be perfectly flat, this introduces a systematic offset of the type expressed by (6). It is important

that this residual slope in the detector remain fixed in order to assure long-term stability and reproducibility. As noted below in Section VI-C, it may be desirable to make a detector with a specific slope which can be used to compensate the frequency shift due to pressure.

It is critically important to null the fundamental frequency signal component ( $v_m$ ) at the detector for another reason. If this is not done, then a signal at  $v_m$  can mix in the detector with the rather strong signals at  $2v_m$  and  $4v_m$  to give signals at  $3v_m$  and  $5v_m$  which gives further offsets. These offsets are avoided by exactly nulling the fundamental signal component of the detected output.

Finally, we must ensure that FM distortion does not occur at the oscillator. For example, second-harmonic FM distortion [19] due to a signal component of frequency  $2v_m$  at the FM input causes a signal component at  $3v_m$  at the detector. This is because the lineshape acts as a mixer which mixes the FM at frequency  $v_m$  with the FM at frequency  $2v_m$  to give a component in the detected output at frequency  $3v_m$  which is then compensated by the normal error signal when the servo is locked. The details of this problem are discussed in [19]; for the ammonia device, the effect of such distortion was minimized (frequency shift less than  $10^{-9}$ ) by ensuring that the second harmonic of the FM input is  $\approx 75$  dB below the fundamental.

### C. Servo Phase Comparators and Integrators

Conventional analog phase comparators have output voltage offsets due to asymmetries which may exist in the signal switching portion of the device. For the ammonia device the signal from the microwave detector undergoes a  $180^\circ$ -phase reversal at each half-cycle of the reference signal

(third or fifth harmonic of modulation frequency). The signal path through the comparator for one half-cycle versus the other half-cycle must be identical to realize zero offset; however, this is difficult to achieve and therefore offsets will exist. These offsets not only affect the accuracy of the locked oscillator, but also the stability, since they are observed to change in time.

The phase comparator is followed by an integrator to realize a second-order loop filter. Analog integrators suffer from input voltage offsets. Furthermore, the common analog integrators, having a capacitor in the negative feedback path, have finite dc gain set by the amplifier; a practical limit is about 140 dB. Capacitor leakage also degrades the analog integrator's performance.

A new phase comparator and integrator was designed and built which employs digital electronics and can directly replace currently used analog circuitry [20]. Since the line-splitting goal in the ammonia standard was high ( $\sim 1 \times 10^{-5}$ ) to achieve  $10^{-10}$  stability and the offset had to be  $\sim 1 \times 10^{-4}$  or lower, there was incentive to pursue techniques other than analog. Virtues of the digital system are:

- 1) negligible voltage offset
- 2) no capacitor, hence no leakage
- 3) infinite gain at dc
- 4) excellent low-pass filter characteristics
- 5) excellent environmental immunity.

These positive aspects were weighed against the following observed shortcomings:

- 1) lower modulation rates necessary
- 2) quantization noise (additive white noise).

At modulation frequencies exceeding a few kilohertz, the analog comparator and integrator begins to outperform the digital integrator with regard to usable feedback gain and additive noise. Therefore, the best servo for the ammonia device would be designed using both analog and digital techniques: The analog portion to respond in short term (e.g., for times less than about one second) and the digital portion to respond in long term (e.g., greater than one second).

## VI. RESULTS

### A. Stability

A plot of the frequency stability obtained with the ammonia based oscillator is shown in Fig. 2. These data were computed using the two sample variance for different averaging times [4]; frequency drift has not been removed. The results using the free running  $\sim 0.5$ -GHz stripline oscillator have been discussed in Section II above. The data shown for  $10^{-2}$  s to 10 s were taken with the oscillator locked to the apparent line center using third harmonic ( $3\nu_m$ ) dispersion lock discussed in Section V; the cavity was unlocked for this data. The longer term data (10 s to  $6 \times 10^3$  s) were taken with the complete system shown in Fig. 4 using a cell volume of  $230 \text{ cm}^3$  to increase signal strength. In both cases data

were taken with a gas flow system in order to directly monitor pressure; the basic problems of frequency stability and cell-cavity design were separated to simplify development.

The shorter term data were taken with a small cell ( $25 \text{ cm}^3$ ) to illustrate the relatively good stability obtained with small cell sizes. When the short term data (locking only the oscillator) were taken with the larger cell ( $230 \text{ cm}^3$ ), approximately a factor of five improvement in stability was observed between  $10^{-2}$  s and 1 s. The cause of the flicker behavior (flattening of the  $\sigma_y(\tau)$  curve) is not understood at this time but is perhaps related to instabilities in the control of the lineshape distortion mechanisms (Section V).

### B. Accuracy

For the reasons outlined in Section VI-C below, the obtained accuracy will depend on system parameters such as ammonia pressure and detector slope. Since we are really interested in frequency reproducibility between units and over long periods of time (years), the reproducibility and stability of these system parameters is of primary importance. We estimate that the accuracy obtained in the above sense is approximately  $\pm 2 \times 10^{-9}$  if the detector slope can be held to  $\pm 2$  percent of its initially set value. This estimate is explained below; data are still needed in very long term and for different units.

### C. Systematic Frequency Offsets

In our system, the two most important systematic frequency shifts were those due to ammonia pressure and detector slope. Assuming the detected fundamental (signal at  $\nu_m$ ) has been electronically nulled, then there can still be a systematic offset if the detector is not flat; this offset is expressed by (6) where  $\beta$  is the AM of the source and where we have assumed that the total detected signal is much larger than that due to the ammonia ( $\gamma \ll 1$ ). (This is the case except when the cell is very long ( $\sim 10 \text{ m}$ ) and/or the reflection coefficients at the cell-cavity interfaces are very high.) In previous work [3], [8], [21];  $\Delta\nu_t$  has been expressed by the semiempirical relation:

$$\Delta\nu_t = [(\Delta\nu_0)^2 + (\Delta\nu_p)^2]^{1/2} \quad (7)$$

where  $\Delta\nu_0$  ( $\sim 100 \text{ kHz}$ ) is the line broadening due to all causes (primarily Doppler effect) except for ammonia-ammonia collisions, and  $\Delta\nu_p$  is the linewidth due to collisions (pressure).

The frequency shift due to pressure is written as:

$$\delta\nu_p = \alpha\Delta\nu_p$$

where  $\alpha \simeq 0.01$  [22]. Therefore, the total shift due to detector slope and pressure is given by:

$$\delta\nu = -\beta[(\Delta\nu_0)^2 + (\Delta\nu_p)^2]^{1/2} + \alpha\Delta\nu_p \quad (8)$$

The important point to note is that at high pressure ( $\Delta\nu_p \gg \Delta\nu_0$ ) we have:

$$\frac{\partial(\delta\nu)}{\partial\Delta\nu_p} \cong -\beta + \alpha.$$

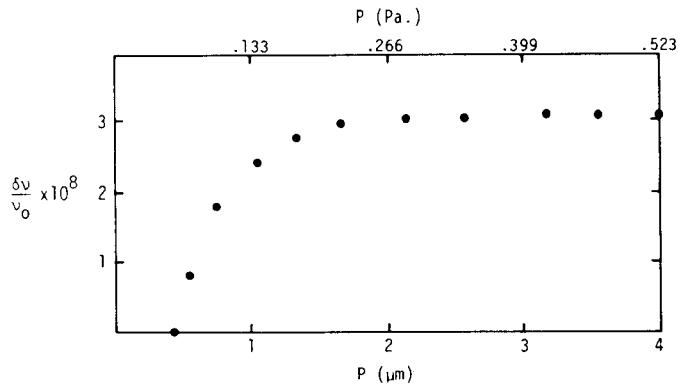


Fig. 5. Fractional frequency offset (from arbitrary reference) versus pressure. (Absolute pressure known to only a factor of two.)

Therefore, if  $\beta \cong \alpha$ , then the change in frequency with change in pressure is very small, therefore reducing pressure (and temperature) shifts. If  $\beta = \alpha$ , and when  $\Delta v_p \ll \Delta v_0$ , then  $\partial(\delta v)/\partial \Delta v_p \cong \alpha$ . Experimental verification of this is given in Fig. 5 where we have plotted fractional frequency offset (from an arbitrary reference point) versus pressure. We note that at high pressure ( $P \cong 0.2$  Pa) a factor of 2 change in pressure gave a fractional change in output frequency of less than  $10^{-9}$ . However, we observed at high pressure that the output frequency is in error about  $4 \times 10^{-9}$  from the value of  $v_0$  which is predicted by (8).

Nevertheless, we could hope to set the detector slope so that  $\beta \cong \alpha$  and greatly reduce pressure (and temperature) sensitivity. If  $\beta$  changes, however, then the frequency would change so that at high pressure ( $\Delta v_p > \Delta v_0$ ):

$$\frac{\partial(\delta v/v_0)}{\partial \beta/\beta} \cong -\beta \frac{\Delta v_p}{v_0}$$

If  $\Delta v_p \cong 230$  kHz,  $\beta \cong \alpha = 0.01$ , then if  $\beta$  changed by 2 percent, the output frequency would change by  $\sim 2 \times 10^{-9}$ . More work is needed to improve the above scheme and of course other pressure compensation methods are possible.

#### D. Ammonia Containment

Work with ammonia cells needs further development but first results were encouraging. For both types of cells the pressure appeared to stabilize about two days after sealing the cell. (Observed signal strength dropped 30 percent during this period.) These first results indicated that the stainless steel waveguide cells were slightly better, and following the first two days, signal degradation was less than ten percent after a few weeks. Future work is needed to ensure cleanliness and integrity of the cells, and better results could be anticipated (see Section VI-F2) below).

#### E. Integrator-Demodulator Stability

The analog and digital demodulators can both be set to give initial offsets corresponding to frequency inaccuracies of less than  $10^{-10}$ . Therefore, it is critical that their drift be minimal. To check this, the system was first locked using the digital servoes. The  $3v_m$ -error signals were then applied to

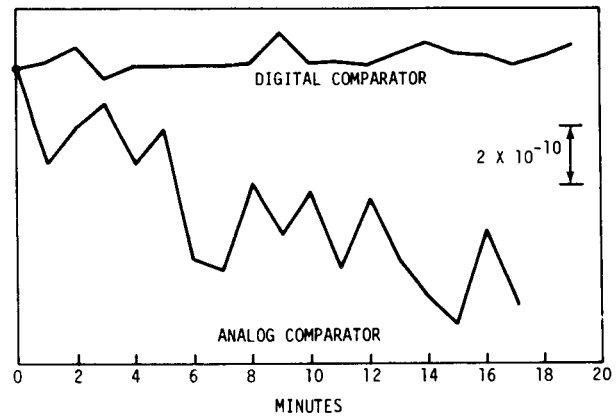


Fig. 6. Drift of analog and digital comparator (demodulator) in time. Vertical scale calibrated in terms of equivalent frequency offset (error) introduced by comparator.

the inputs of separate digital and analog demodulators, and the dc outputs were monitored in time. If no drifts exist in these separate demodulators the output should remain constant in time. Fig. 6 shows the results of a typical measurement of this kind. The analog demodulator was the better of two commercially available high performance lockin amplifiers. Over a 20-min period, the digital offset drift was smaller by more than an order of magnitude over the analog offset drift. The vertical scale in Fig. 6 is calibrated in terms of the equivalent fractional frequency offset of the primary oscillator; it therefore demonstrated that the digital system was adequate.

#### F. Environmental Sensitivity

1) *Vibration Sensitivity*: Because of the fast servo attack time provided in the ammonia standard, sensitivity to vibration should be low. This is true to the extent that the apparent absorption line is stable and that there is sufficient servo gain at the vibration frequency.

The potential effect of vibration suppression can be seen by observing the spectral density of phase fluctuations  $S_\phi(f)$  of the 0.5-GHz oscillator under vibration. An example of such a measurement is shown in Fig. 7; one curve showed the oscillator locked to the ammonia and the other with it unlocked. (Note however that the microwave cavity was *not* vibrated.) Vibration frequency was 40-Hz sine with a peak acceleration of  $5 \text{ m/s}^2$  (unity gain frequency  $\cong 1$  kHz). We see at least 45-dB reduction of the power in the 40-Hz additive phase spectral component when the oscillator is locked. This represented an acceleration sensitivity of at most  $5 \times 10^{-11} \text{ s}^2/\text{m}$  ( $5 \times 10^{-10} \text{ g}$ ).

In a systems design, it would be desirable to build and mount the oscillator so that vibration sensitivity is as low as possible for vibration frequencies outside the servo loop bandwidth. Since the bandwidth can be made wide in the case of the  $\text{NH}_3$  standard (approaching 100 kHz), some flexibility exists in the choice of the oscillator's mechanical design and supporting structures (see Section II).

2) *Temperature Sensitivity*: Temperature will vary the most critical parameters affecting accuracy and long-term

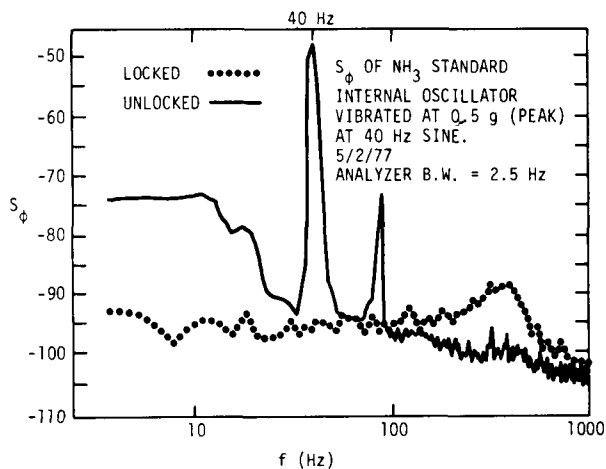


Fig. 7. Plot of phase spectral density  $S_\phi(f)$  for locked and unlocked  $\sim 0.5$  GHz oscillator which is vibrated with a 40-Hz sine wave having a peak acceleration of  $5 \text{ m/s}^2$ .

stability; i.e., pressure and detector slope (see Section VI-C). Data was not taken on detector slope; however, to obtain  $\pm 2 \times 10^{-9}$  accuracy, the slope of the detector must be maintained to about 2 percent over the operating temperature of the device (see Section VI-C).

Pressure dependence on temperature was estimated by measuring signal strength as a function of temperature on the sealed stainless-steel waveguide. In this way we observed a sensitivity of  $1/P \partial P/\partial T \cong 0.05/^\circ\text{C}$ . That is, a change of 5 percent in pressure was observed for a change in temperature of  $1^\circ\text{C}$ . If the compensation scheme of Section VI-C is used, this gives a temperature coefficient of  $\leq 5 \times 10^{-11}/^\circ\text{C}$ . However, for good accuracy and stability at low ambient temperatures, some minimal temperature servoing would be required. For example, we could servo the temperature to give a fixed second harmonic signal at the detector.

3) *Electric and Magnetic Field Sensitivity*: Electric fields are only of importance in the construction details of the gas cell where thermoelectric and contact potential problems may be present. A worst estimate can be based on the most sensitive hyperfine component of the (3-3) line; for this we have a relative shift of about  $10^{-9}E^2$  ( $E$  in  $\text{V/cm}$ ). Since electric fields surely can be limited to less than  $0.1 \text{ V/cm}$ , this does not appear to be a problem.

To first order, application of magnetic fields causes only a broadening of the ammonia line. This broadening has been observed to be [3]

$$\frac{\partial(\Delta\nu_i)}{\partial B} = 7 \times 10^3 \text{ kHz/T.}$$

If the pressure shift compensation scheme of Section VI-C is used, then a residual frequency shift due to magnetic field will exist

$$\begin{aligned} \frac{1}{\nu_0} \frac{\partial(\delta\nu)}{\partial B} &\simeq \frac{1}{\nu_0} \frac{\partial(\delta\nu)}{\partial(\Delta\nu_i)} \frac{\partial(\Delta\nu_i)}{\partial B} = 3 \times 10^{-4} \alpha/\text{T} \\ &= 3 \times 10^{-6}/\text{T.} \end{aligned}$$

Therefore in extreme magnetic-field environments some simple magnetic shielding may be required. The second-order Zeeman effect is extremely small; the relative shift is about  $2 \times 10^{-7} B^2$  ( $B$  in Tesla) and is, therefore, negligible [11].

### VII. FUTURE PROJECTIONS

In this work a fully integrated prototype was not constructed; and for simplicity the separate aspects of the device were investigated individually. However, some estimates of physical parameters can be made based on present results.

a) *Size Requirements*: The lower limit on size will primarily be limited by the size of the ammonia cell. It is expected that the cell should occupy no more than 1-liter volume; hence the overall package may be from 1–2 liters in volume.

b) *Weight Requirement*: With proper choice of materials the expected final package weight should be less than 2 kg. For operation in extreme magnetic fields, shielding may have to be included; this will increase weight by approximately  $\frac{1}{2}$  kg.

c) *Power Requirements*: The basic electronic components of the present configuration are shown in Fig. 4.

The power requirements for specific portions were:

1) 0.5-GHz oscillator, 0.5-GHz amplifier with multiplier	5.5 W
2) divider chain ( $\div 100$ )	1.0 W
3) detector amplifier and servoes	1.0 W
<b>Total</b>	<b>7.5 W</b>

Reduction in these power requirements could be expected.

### VIII. CONCLUSIONS

Although the results obtained with the present device are encouraging, we could hope for better results with future development. At this time it is difficult to comment on the commercial feasibility of such a device; first, more basic research is required in the area of cell construction.

The largest uncertainties exist in the control of the AM distortion (detector slope) and pressure shift; efforts should be concentrated in these areas. It should be noted that it is possible to use different approaches for these problems. For example, we could modulate the source at two different frequencies and/or with different amplitude; this would allow independent servoing of the detector slope to zero, thus eliminating AM distortion entirely. (Similar to the method of third and fifth harmonic locks used to servo the oscillator and cavity). One is then left with the raw pressure shift which could be compensated in the output frequency by, for example, applying a calibrated correction voltage at the integrator input based on the observed signal amplitude.

### ACKNOWLEDGMENT

We wish to thank the other members of the Frequency and Time Standards Section of NBS for their help and encouragement; in particular H. E. Bell gave much help in the construction of the physical components. We thank F. L.

Walls, S. R. Stein, R. M. Garvey, S. Jarvis, Jr., A. S. Risley, and T. C. English and P. Kwon of Efratom, Inc., for useful ideas and encouragement during the course of the work.

#### REFERENCES

- [1] D. J. Wineland, D. A. Howe, and H. Hellwig, "Special purpose atomic (molecular) standard," in *Proc. 8th Annu. Precise Time and Time Interval (PPTI) Planning Meet.*, pp. 429-447, Dec. 1976.
- [2] H. Lyons, "Spectral lines as frequency standards," *Ann. NY Acad. Sci.*, vol. 55, pp. 831-871, 1952.
- [3] K. Shimoda, "Atomic clocks and frequency standard on ammonia line I and III," *J. Phys. Soc. Jap.*, vol. 9, pp. 378-386 and pp. 567-575, June 1954.
- [4] D. W. Allan, "Statistics of atomic frequency standards," *Proc. IEEE*, vol. 54, pp. 221-230, Feb. 1966.
- [5] G. Hodowanec, "Microwave transistor oscillators," RCA Appl. Note AN 6291.
- [6] E. Oxner, "High performance FETs in low noise oscillators," Siliconix, Inc., Dec. 1973.
- [7] See for example, "Ku-band step recovery multipliers;" also: "Harmonic generation using step recovery diodes and SRD modules," Hewlett-Packard Company, 620 Page Mill Road, Palo Alto, CA, Hewlett-Packard Applications Note 928.
- [8] C. H. Townes and A. L. Schawlow, *Microwave Spectroscopy*. New York: McGraw-Hill, 1955.
- [9] M. S. Cord, M. S. Lojko, and J. D. Peterson, "Microwave spectral tables," NBS Monograph 70, vol. 5, 1968.
- [10] J. De Prins, "Characteristics of the  $N^{15}H_3$  masers," in *Proc. Frequency Standards & Metrology Seminar*, pp. 147-148, Laval Univ., Aug. 1971.
- [11] ———, " $N^{15}H_3$  double beam maser as a primary frequency standard," *IRE Trans. Instrum.*, vol. I-11, pp. 200-203, Dec. 1962.
- [12] S. G. Kukolich, "Measurement of ammonia hyperfine structure with a 2-cavity maser," *Phys. Rev.*, vol. 156, no. 1, pp. 83-92, Apr. 1967.
- [13] D. O. Hayward and B. M. W. Trapnell, *Chemisorption*, 2nd ed. Washington, DC: Butterworths, 1964, pp. 205-248.
- [14] J. Vennet, C. Audoin, and M. Desaintfuscien, "Cavity pulling in passive frequency standards," *IEEE Trans. Instrum. Meas.*, vol. IM-21, pp. 204-209, Aug. 1972.
- [15] The length of the waveguide between reflection points must be approximately equal to an integral number of half-wavelengths.
- [16] F. L. Walls, "Design and results from a prototype passive hydrogen maser frequency standard," in *Proc. 8th Annual Precise Time and Time Interval (PTTI) Planning Meeting*, pp. 369-380, Dec. 1976.
- [17] See for example: H. Hellwig, "Atomic frequency standards: A survey," *Proc. IEEE*, vol. 63, no. 2, pp. 212-229, Feb. 1975; C. Audoin and J. Vanier, "Atomic frequency standards and clocks," *J. Phys. E: Sci. Instr.*, vol. 9, pp. 697-720, 1976.
- [18] A. D. Wallard, *J. Phys. E.*, vol. 5, pp. 927-930, 1972.
- [19] J. M. Shirley, "Some causes of resonant frequency shifts in atomic beam machines, II. The effect of slow frequency modulation on the Ramsey line shape," *J. Appl. Phys.*, vol. 34, pp. 789-791, 1963.
- [20] D. A. Howe and F. L. Walls, "Digital comparator and integrator," in preparation.
- [21] A more exact treatment when both pressure and Doppler effects are important has been given by R. W. Parsons and J. A. Roberts, "The Doppler contribution to microwave line widths," *J. Mol. Spectrosc.*, vol. 18, pp. 412-417, 1965.
- [22] P. L. Hewitt and R. W. Parsons, "Collision broadening and shifting in the inversion spectrum of  $NH_3$ ," *Phys. Lett.*, vol. 45A, no. 1, pp. 21-22, Aug. 1973.